

2014

# Relationship between primary liver hepatocellular carcinoma volumes on portal-venous phase CT imaging

---

<https://hdl.handle.net/2144/15388>

*"Downloaded from OpenBU. Boston University's institutional repository."*

BOSTON UNIVERSITY  
SCHOOL OF MEDICINE

Thesis

**RELATIONSHIP BETWEEN PRIMARY LIVER HEPATOCELLULAR  
CARCINOMA VOLUMES ON PORTAL-VENOUS PHASE CT IMAGING**

by

**EHIMEN AISABORHALE**

B.S., University of Detroit Mercy, 2011

Submitted in partial fulfillment of the  
requirements for the degree of  
Master of Science

2014

© 2014 by  
Ehimen Aisaborhale  
All rights reserved

Approved by

First Reader

---

Hernán Jara, Ph.D.  
Professor of Radiology

Second Reader

---

Stephan Anderson, M.D.  
Associate Professor of Radiology

## **ACKNOWLEDGMENTS**

I am grateful to Dr. Hernán Jara and Dr. Stephan Anderson for their guidance and insight which helped shaped the direction which led to this project being possible. Also, I thank Boston University and its affiliate hospital – Boston Medical Center for providing resources that made this research project possible.

**RELATIONSHIP BETWEEN PRIMARY LIVER HEPATOCELLULAR  
CARCINOMA VOLUMES ON PORTAL- VENOUS PHASE CT IMAGING**

**EHIMEN AISABORHALE**

**ABSTRACT**

The liver is an important organ in the body. It is located under the rib cage on the right side. The liver performs many important functions, it processes food for nutrients that the body requires and also helps in the detoxification of harmful materials. Like any organ in the body, the liver is susceptible to diseases such as liver cancer. Liver cancer is the growth and spread of unhealthy cells of the liver. There are several risk factor for liver cancer, these are: Cirrhosis (scarring of the liver), long term hepatitis B and hepatitis C infection and diabetes patients with long term drinking problem. Hepatocellular Carcinoma is the most common form of liver cancer in adult population which begins in the main type of liver cell (hepatocyte). Because Hepatocellular carcinoma starts from the primary liver cell itself (hepatocytes), as such it is a primary liver cancer. About 30,000 Americans are diagnosed with primary liver cancer yearly, making it an important disease that plaques our society and therefore needs proper diagnosis.

In clinical evaluation of primary liver cancer such as HCC, the use of medical imaging technology has been commonplace. Most medical facilities across the country and globally typically use Computed Tomography (CT) and/or Magnetic Resonance

Imaging (MRI) in the diagnosis and treatment follow up of Hepatocellular carcinoma. The medical imaging devices are used to determine the extent and volume of the tumor of the cancerous liver cells. In clinical trials involving the imaging of HCC tumors, the typical protocol used in the CT imaging of HCC involves the use of contrast enhanced dual phase acquisition. This approach is based on the physiology of the blood flow through the liver. Since HCC tumors are hypervascular in nature, it would thus be more apparent in the arterial phase of an acquired CT image. The aforementioned characteristic was tested with a volume paradigm which measure and compare the volume of both the arterial phase and portal venous phase acquired images in the experiment. Overall this study helps in furthering goals to reduce the patient dose from the x-ray tubes during clinical trials. The results of the experiments ( $n = 19$ ,  $t = 0.67$ ,  $p = 0.26$ ), indicates no significant difference between the volume of the HCC tumor images acquired both in the AP and PVP.

## TABLE OF CONTENTS

|  |     |
|--|-----|
| TITLE.....                               | i   |
| COPYRIGHT PAGE.....                      | ii  |
| READER APPROVAL PAGE.....                | iii |
| ACKNOWLEDGMENTS .....                    | iv  |
| ABSTRACT.....                            | v   |
| TABLE OF CONTENTS.....                   | vii |
| LIST OF TABLES .....                     | ix  |
| LIST OF FIGURES .....                    | x   |
| LIST OF ABBREVIATIONS.....               | xi  |
| INTRODUCTION .....                       | 1   |
| <b>Subsection One (Background)</b> ..... | 4   |
| <b>Subsection Two (Theory)</b> .....     | 8   |
| METHODS (research-based).....            | 10  |
| RESULTS .....                            | 15  |
| DISCUSSION.....                          | 20  |
| CONCLUSION.....                          | 22  |
| REFERENCES .....                         | 23  |

CURRICULUM VITAE..... 26

## LIST OF TABLES

| Table | Title  | Page |
|-------|--|------|
| 1     | Data for the computed volume of two individually measured ROI of HCC tumors in both arterial and portal venous phase CT image. | 15   |
| 2     | The average volume of the segmented tumors from both the AP and PVP.   | 16   |
| 3     | Mean deviations for the dual volume measurements of the AP tumors.   | 17   |
| 4     | Mean deviations for the dual volume measurements of the PVP tumors.  | 18   |
| 5     | Output of the computed simple right tail t-test of the AP and PVP liver tumor volumes.   | 19   |

## LIST OF FIGURES

| Figure | Title   | Page |
|--------|---|------|
| 1      | Example of an Arterial Phase Image.   | 3    |
| 2      | Example of a Portal Phase Image.  | 3    |
| 3      | Process of importing images on to the ImageJ Software Platform.                             | 12   |
| 4      | The freehand selection tool for drawing ROI on images loaded on ImageJ.                     | 13   |
| 5      | Example ROI drawn on an HCC tumors with the freehand selection tool.                        | 13   |
| 6      | The tabulated output of a processed selected ROI of an image loaded on the ImageJ platform. | 14   |

## LIST OF ABBREVIATIONS

|            |  |
|------------|--|
| AP.....    | Arterial Phase                                 |
| BMC.....   | Boston Medical Center                          |
| CT.....    | Computed Tomography                            |
| DICOM..... | Digital Imaging and Communications in Medicine |
| HCC.....   | Hepatocellular Carcinoma                       |
| IV.....    | Intravenous                                    |
| kVp.....   | Kilo Voltage Peak                              |
| MA.....    | Milli Ampere                                   |
| MHU.....   | Million Heat Units                             |
| MRI.....   | Magnetic Resonance Imaging                     |
| PACS.....  | Picture Archiving Communication Systems        |
| PVP.....   | Portal Venous Phase                            |

## INTRODUCTION

The liver is not only one of the largest organs in the human body; it is also one of the most important organs in the body. The liver helps the body filter harmful substances from the blood and makes substances that help to digest food to produce energy reserves for the body. Proper functioning of the liver thus is inherent to overall functioning of the body. However, the liver is prone to diseases just like most organs in the body. Primary liver cancer is a form of cancer that starts in the liver and may spread to other parts of the body. Such type of liver cancer is hepatocellular carcinoma which is the most common type of primary liver cancer. Hepatocellular Carcinoma's (HCC) has no unique cause, but it is secondary to other liver diseases such as viral hepatitis and cirrhosis. Treatment for HCC's varies depending on the prognosis of individuals who have this disease based on their doctor's evaluation. Overall, treatment options for HCC depend on the size of the tumor. The advent of medical imaging technology has been tremendously important to staging of this disease by measuring the size of the tumor.

Different types of imaging modalities are used for the evaluation of HCC tumors in the liver; importantly is the Computed Tomography that has the advantage of being very fast and gives good soft tissue contrast when combined with intravenous administration of an exogenous contrast material injection. Dual phase contrast enhanced CT imaging has been a very important procedure used by physicians to scout patients liver for potential tumors during clinical trials. Dual phase imaging is particularly useful for liver imaging based on the physiology of this organ. The two phases in which the images are acquired are the hepatic arterial phase and the hepatic venous phase. The

phases are named based on the vessels that supply the blood to the liver at specific times at which it takes an intravenously injected iodine contrast bolus to get to the liver. The hepatic artery delivers 20-25% of blood flow to the liver while the portal vein delivers the remaining 75-80%. During a dual phase imaging of the liver, post injection of an intravenous iodine contrast bolus, the effect of the contrast material delivered to the liver via the hepatic artery will be seen approximately 20-30 seconds while that of the portal vein will be seen at about 45-55 seconds. The blood flowing through the portal vein takes a little longer to get to the liver because it has to circulate through the spleen and mesentery before reaching the liver.

Not only is CT an imaging modality used in clinical evaluation of abdominal diseases due to its ability to show contrast between soft tissues, importantly, it can help differentiate different types of tumors associated with the liver. Hypervascular tumors such as hepatocellular carcinoma are more distinct and well delineated in the arterial phase of CT image acquisition post contrast injection. However, hypovascular tumors are not distinct and well delineated in the arterial phase of acquisition.

In the venous phase of the contrast enhanced CT images, the reverse is the case, as hypovascular focal tumors are more distinct in comparison to the rest of the liver parenchyma.

When an intravenous contrast bolus is injected to the blood stream, the contrast material is delivered to the hepatic artery, and will be seen approximately 20-35 seconds before the effect of the contrast material delivered by the portal vein will be seen at 35-45 seconds. The concentrated level of the injected contrast in the arterial blood flow

opacifies the images of tumors in such phase, in comparison to the parenchyma background making them more visible and well delineated. Since we know that HCC tumors are inherently well differentiated and delineated in the arterial phase of a contrast enhanced dual phase CT image, this thesis work compares and evaluate the volume of HCC tumors acquired through both the AP and PVP for clinical trial purpose. The specific parameter being studied in this experiment is the difference in volume of tumor obtained for individual subjects in both the AP and portal PVP of the acquired contrast enhanced CT images. The experimental work seeks to determine if there is a significant difference between the AP and the PVP volumes of an HCC tumor.

For clinical diagnosis and during clinical trials, it is worth noting that abdominal contrast enhanced CT imaging of the liver is also helpful in deciphering other types of potential tumors found both in the different part of the abdominal cavity and importantly in the liver.

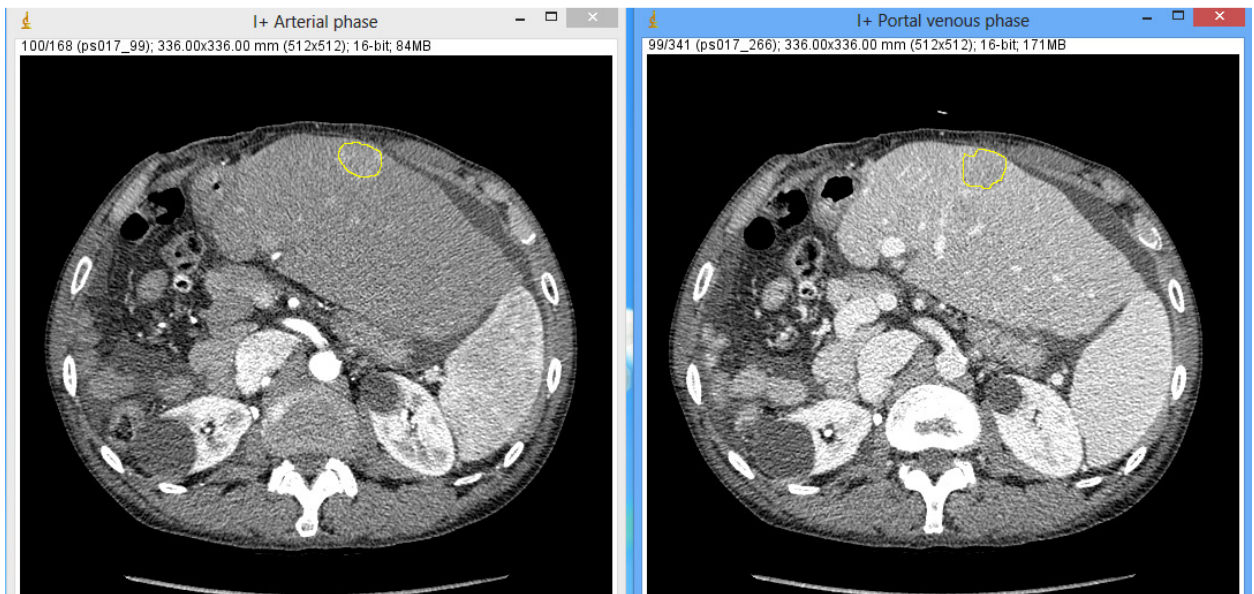


**Figure 1:** Example of a HCC tumor in AP CT Image. **Figure 2:** Example of a HCC tumor in PVP CT Image.

Previous literatures have described the physiology of hypervascular and hypovascular tumors in terms of blood flow and how an injected contrast material will get to the liver within a certain period. Furthermore, these literatures described the difference between hypervascular and hypovascular tumors in terms of how they attenuate in comparison to the background liver parenchyma post contrast injection. Also, some literatures have described the different segmentation algorithms and their shortcomings that could automatically segment hypervascular and hypovascular tumors in a dual phase contrast enhanced CT images. However, there were limited resources that compared the segmented tumors in both the arterial and the portal venous phase in terms volume. This became a springboard for this study, with a primary objective to corroborate tumor size of hypervascular tumors (HCC precisely) of subjects by segmenting its dual phase acquired CT images manually and comparing the volume values of both phases.

If the hypothesis of this study is corroborated with positive experimental results, this research will serve as a background for limiting the x-ray dose patients receives from CT when their HCC tumor is being evaluated for clinical trials.

### **Subsection One (*Background*)**

Computed tomography is a non- invasive imaging device that is used for imaging bones, soft tissues and blood vessels. Computed tomography today is used in the diagnosis of many ailments, as it allows doctors to view slices and cross sections of bones

such as the skull, hemorrhages in blood vessels and importantly tumors in both bones and soft tissues. CT imaging of the liver has been very important in clinical trials during the development of novel therapeutic agents, including those directed at HCC. Most clinical trials involving imaging of liver cancers are based on understanding how cancer tumors respond to therapies by staging the disease through visible changes observed via imaging modalities. CT works similar to an x-ray. The conventional x-ray imaging operates based on the absorption of incident x-rays on a body. These x-rays are focused on a part or section of the body. As the x-rays pass through the body, some x-ray photons will be absorbed by the body, while others will not be absorbed. The non-absorbed or transmitted x-rays that emerge from the body will interact with a detection device and thus form a two-dimensional image of the body part.

CT scanning is very different from the regular projectional x-ray imaging. It differs by the fact that a two dimensional image is acquired and in the manner that the image output is provided by its detector. A typical CT scanner creates a two dimensional cross sectional images (slice) of three dimensional body structure by utilizing a computer based mathematical technique called reconstruction. The CT scan has many important parts that makes acquiring the cross sectional images of a body possible. These parts include the gantry, x-ray tube, collimators, filters, detectors and the data acquisition system.

The first major component of the CT imaging system is the gantry and the patient table or couch. The gantry is a moveable frame that contains the x-ray tube, collimators, filters, detectors and the data acquisition system. It also contains the rotational component

which includes the slip ring systems and all associated electronics such as the gantry angulation motors and positioning laser lights. The slip ring that is found on the gantry of the CT system helps for continuous scanning without interference by cables. Gantry angulation which is manufacturer specific, allows the operator to align pertinent anatomy with the scanning plane. The opening that allows patient access to the CT scanner through the gantry is known as the aperture. This aperture varies depending on the manufacturer. Generally, gantry aperture ranges from 50-85 cm while CT's with larger apertures are typically used for special procedures such as large volume biopsy procedures. These larger aperture CT's allow for easy manipulation of biopsy equipment's and as such reduces the risk of injury to the patient during scanning. The entire diameter of the gantry aperture is not the scanning diameter of the CT system; it is lesser than the gantry diameter. Lasers or high intensity lights serve as the anatomical positioning guides that reference the center of the axial, coronal, and sagittal imaging planes of the CT scanner.

The procedures for acquiring CT images, allows for significant radiation exposure factors over a short period of time (high mA and kVp). Advancements in CT designs such as in the case of modern helical/spiral CT allows for continuous scanning while the patient table moves through the gantry. Such continuous scanning leads to the buildup of heat on the x-ray tube and may cause heat stress or possible destruction of the material that makes up the x-ray tube if it does not have a mechanism to dissipate the heat. CT x-ray tubes are designed with materials with high heat capacity so as to allow optimal operation of the tube and avoid operation damage to the tube. In CT, the x-ray tubes are

designed to absorb high heat levels generated from the high speed rotation of the anode and the bombardment of electrons upon the anode surface. Modern CT systems are designed with x-ray tubes with heat capacity of 3.5 to 5 million heat units (MHU).

For the CT scanners to be able to operate continuously without interruptions due to overheating, the x-ray tubes must possess the capacity to dissipate heat at a high rate. Most CT tubes utilize oil and air cooling system to eliminate heat and allow for continuous proper functioning of the x-ray tube. In addition, the CT anode has a large diameter with graphite backing that allows it to absorb and dissipate a large amount of heat.

When x-ray beams travel through the patient, these are attenuated by the anatomical structures it passes through. Unlike conventional x-rays that utilize a film screen system as its primary image receptor to collect the attenuation information, CT beam is collected on a detector. The CT process relies on the collection of attenuated photon energy and converting them to an electrical signal, which will be further converted to digital signal for computer reconstruction.

### **Subsection Two (*Theory*)**

The detection of liver masses in CT imaging is based on the x-ray attenuation difference between the tumor and the normal liver mass. Liver tumors may not be visible in non-contrast enhanced CT because the inherent contrast between the tumor and the surrounding liver parenchyma is too low. An intravenous (IV) contrast is needed to increase the conspicuity of tumor. There is a dual supply of blood to the liver; the blood supply to the normal liver parenchyma is supplied by the hepatic artery (approx. -75%) and the portal vein (approx. -25%). In case of a normal liver with an infusion of the IV contrast, the liver would enhance maximally in the portal venous phase. All liver tumors receive the majority of their blood supply from the hepatic arterial system, so when they enhance, it will be in the arterial phase. The difference in blood supply to the liver, leads to different enhancement patterns between the liver tumors and normal liver parenchyma in different phases of the enhancement.

In the arterial phase of enhanced CT imaging of the liver, hypervascular tumors are enhanced via the hepatic artery before the rest of the surrounding parenchyma enhances. This is because contrast is not yet in the portal venous system. The enhancement of the hypervascular tumor in the arterial phase of its enhancement makes it visible as an area of hyperattenuation compared to the relative hypoattenuation of the rest of the liver. But when the surrounding liver parenchyma starts to enhance in the portal venous phase, the hypervascular tumors may start to be obscured.

During the portal venous phase, hypovascular tumors are detected when the normal parenchyma of the liver enhances completely. The hypovascular tumors will be visible as hypodense tumors in a relatively hyperdense liver.

For the optimal enhancement of hypervascular tumors, optimal timing of the scan and the speed of the contrast injection are very important. The infusion of an IV contrast into the liver during arterial phase CT imaging will see the blood containing the contrast material enhancing the tumor from about 20 seconds to 30 seconds. The early phase of the enhancement starts at about 18 seconds and as such the tumor is not hyperdense compared to its liver parenchyma. At 35 seconds – late arterial/early portal venous enhancement, maximum enhancement of the hypervascular tumors is achieved, as it becomes hyperdense compared to the rest of the liver parenchyma. At the late arterial enhancement (35 seconds), the portal venous system starts to enhance, until the entire liver is concentrated with the contrast at the late portal venous enhancement - 75 seconds. At this point characterized hypovascular tumors become visible.

## **METHODS (research-based)**

This retrospective research study includes abdominal CT images of patients who were diagnosed with focal HCC at the Boston Medical Center (BMC). The CT images for this study are from patients who have undergone a dual phase contrast enhanced CT images within the past 10 years. The images were acquired under the BMC standard liver imaging protocol of 1.25 mm slice selection thickness. The data sets obtained from the CT images of the patients for this research included both males and female patients. While there was no age restriction on the subjects used, the sample population for this research was entirely adult based as a result of pathological conditions that limits hepatocellular carcinoma mostly to adult populations. There was variation in the race and ethnicity of the subjects associated with the data set used for this research.

The inclusion criteria for this research are individual subject images of pathologically diagnosed HCC focal tumors that are visible and well circumscribed in both the arterial and portal venous phase of a contrast enhanced dual phase CT images, while the exclusion criteria are patients whose image contains multiple tumors. For this project, the intended number of subjects was 20, as that was within the range of subject used in similar experiments. Over 30 dual phase abdominal CT images of patients with focal HCC was examined for this experiment, with 19 meeting the inclusion criteria. The experimental design for this research was simple and straightforward. The images used in acquiring data for this research was first de-identified with a specialized DICOM de-identifier program before they were screened for both inclusion and exclusion factors. After the aforementioned steps were taken, the identified tumors in both phases of

acquisition were then segmented manually using “ImageJ” software. The ImageJ software is an open source image processing software that is created and made available by the National Institute of Health (NIH). This software is used in the segmentation of individual tumors and overall in the determination of the volume of these tumors. Each subject that was included in this research was assigned a number; the subjects range from P1 through P19. The segmentation was done twice for each phase of the image acquisition and the average volume value was then tabulated. There was no control group in this experiment; however the control factor used was that the slice selection for segmentation in each phase was the same for the repeated segmentation.

### **Subsection One (Image Processing)**

In processing the images that were available for this research, the images were first identified to meet the initial criteria of being an HCC tumor that is well circumscribed by Dr. Stephan Anderson and made available through the Boston Medical Center (BMC) picture archiving communication system (PACS). The images were downloaded on a secure system and instantly de-identified using DICOM anonymizer PRO software. All the downloaded images were then reviewed for inclusion criteria. The images that met the inclusion criteria were downloaded, divided into the arterial and venous phases of the acquisition and further saved in folders named by their respective acquisition phases. Both folders were subsequently saved into a supra-folder that was named with their individual subject identification numbers. The images were processed

by uploading individual images on the ImageJ platform. Uploading the images on the ImageJ platform was accomplished by clicking on file menu on the ImageJ platform, under the file menu, the import command was clicked. The location of the folder containing the images was located and the specific folder needed to be processed uploaded.

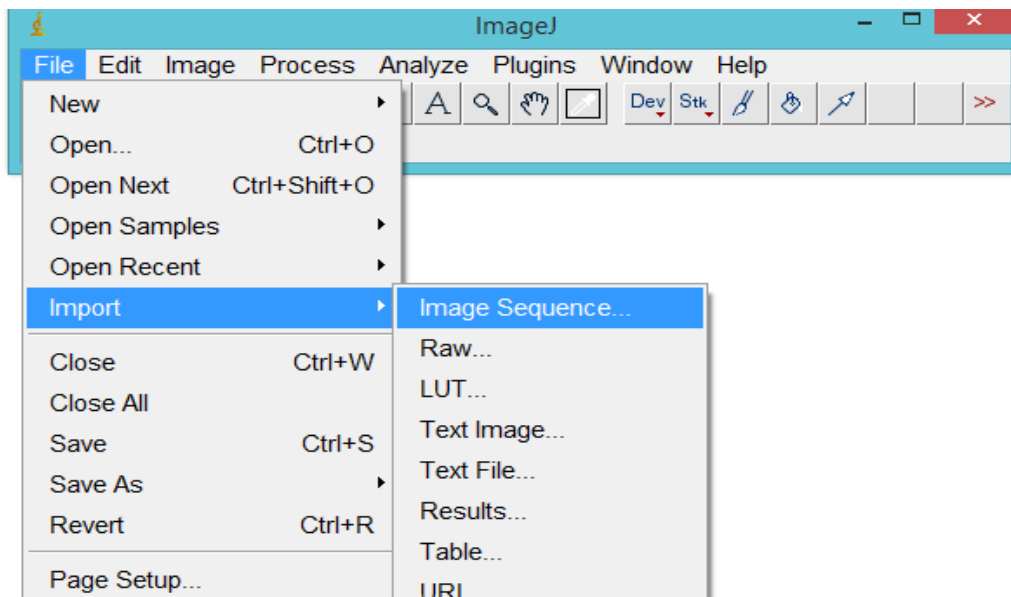


**Figure 3:** Process of importing images on to the ImageJ Software Platform

Once the specific image was uploaded on the ImageJ platform, the software downloads all the image slices on one moveable panel. The images were inspected through for a visible HCC tumor that is well circumscribed. When the tumor was identified, it was segmented in multiple slice panels if visible on multiple subsequent panel.

The segmentation was performed on the ImageJ platform by using the freehand selection tool to manually draw a region of interest (ROI) along the circumference of the tumor at each slice selection.

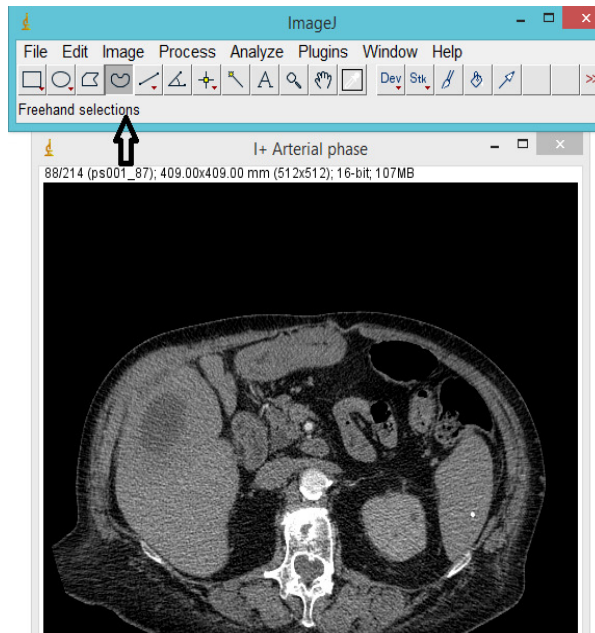


**Figure 4:** The freehand selection tool for drawing ROI on images loaded on ImageJ.

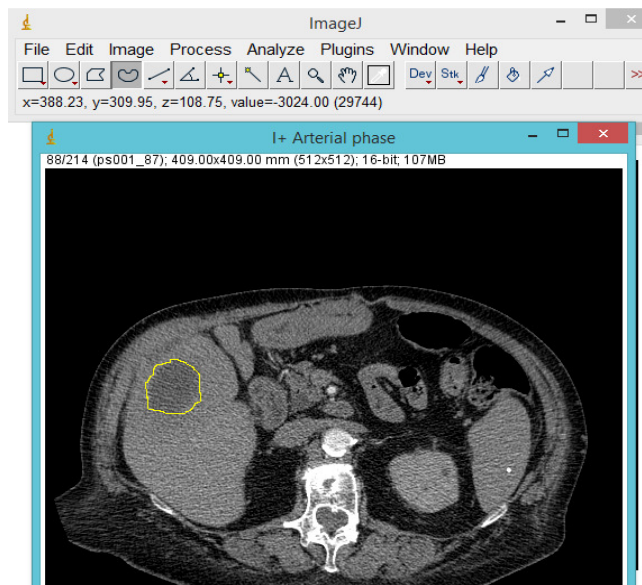
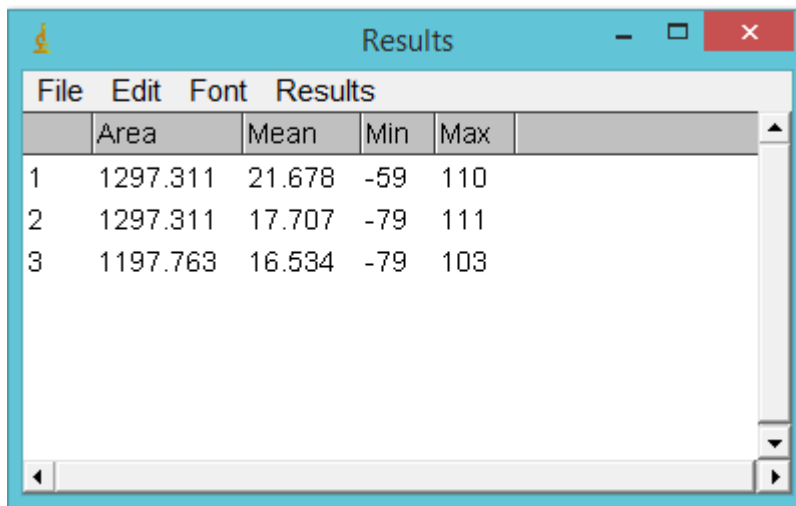


**Figure 5:** Example ROI drawn on an HCC tumors with the freehand selection tool.

Once the selection was done at each slice frame, the data containing the area, of the segmented tumor is computed with the command “ctrl + M” on the ImageJ software

using the keyboard. This displays the tabulated results of the processed image as seen below on figure 5. The areas in the displayed tables were averaged to get the mean values of the individual images for both the arterial and portal venous phases. The mean value obtained from the segmented slices was multiplied by the slice thickness (1.25 mm) and the number of slides which an ROI was acquired in order to determine the mean volume in (mm<sup>3</sup>). The mean volumes were converted to cm<sup>3</sup> by dividing the numbers by 1000. This was done in order to lessen the digits and make it easy to statistically analyze the data.



The screenshot shows a window titled 'Results' with a menu bar containing 'File', 'Edit', 'Font', and 'Results'. Below the menu bar is a table with the following data:

|   | Area     | Mean   | Min | Max |
|---|----------|--------|-----|-----|
| 1 | 1297.311 | 21.678 | -59 | 110 |
| 2 | 1297.311 | 17.707 | -79 | 111 |
| 3 | 1197.763 | 16.534 | -79 | 103 |

**Figure 6:** The tabulated output of a processed selected ROI of an image loaded on the ImageJ platform.

## RESULTS

The profound text of my thesis goes here. The profound text of my thesis goes here. The profound text of my thesis goes here. The profound text of my thesis goes here. The profound text of my thesis goes here. The profound text of my thesis goes here.

In the statistical analysis of the data of the area abstracted from the ROI drawn on each tumor on both phases of the HCC images, Microsoft Excel was used in the analysis of these data. In both phases of the image acquisition, the image processing was done twice and the values computed and tabulated in the tables 1 - 5 below.

**Table 1:** Data for the computed volume of two individually measured ROI of HCC tumors in both arterial and portal venous phase CT image.

| Patient | Arterial 1 (cm <sup>3</sup> ) | Arterial 2 (cm <sup>3</sup> ) | Venous 1 (cm <sup>3</sup> ) | Venous 2 (cm <sup>3</sup> ) |
|---------|-------------------------------|-------------------------------|-----------------------------|-----------------------------|
| 1       | 2.04439625                    | 2.20632                       | 3.99467125                  | 4.00185                     |
| 2       | 58.69219                      | 58.2718375                    | 28.7996375                  | 28.3785425                  |
| 3       | 4.1373325                     | 3.83060125                    | 4.65458125                  | 4.27165                     |
| 4       | 0.663385                      | 0.691545                      | 2.337825                    | 2.29071125                  |
| 5       | 4.46553                       | 4.5315975                     | 3.86496375                  | 3.57199125                  |
| 6       | 0.13339625                    | 0.1287275                     | 0.05602625                  | 0.05869375                  |
| 7       | 13.300805                     | 13.26866875                   | 1.363677917                 | 1.383865417                 |
| 8       | 12.0543375                    | 11.90169625                   | 12.42450875                 | 10.95618375                 |
| 9       | 0.79935375                    | 0.78513625                    | 0.512425                    | 0.50413375                  |
| 10      | 0.69815875                    | 0.68323375                    | 0.57627125                  | 0.60777875                  |
| 11      | 1.36944625                    | 1.35955875                    | 1.375625                    | 1.3181525                   |
| 12      | 0.69832                       | 0.6834875                     | 0.3559575                   | 0.3683175                   |
| 13      | 0.10604                       | 0.1208625                     | 0.09691875                  | 0.078675                    |
| 14      | 0.10604                       | 0.1208625                     | 0.07910125                  | 0.0803375                   |
| 15      | 0.10544                       | 0.10886875                    | 0.0565775                   | 0.05143375                  |
| 16      | 0.17424625                    | 0.2332575                     | 0.1649525                   | 0.213741                    |
| 17      | 2.11832875                    | 2.12909625                    | 1.6074525                   | 1.85131875                  |
| 18      | 0.59927125                    | 0.60238375                    | 0.66231125                  | 0.6662025                   |
| 19      | 0.79099625                    | 0.779825                      | 0.67024625                  | 0.6596075                   |

Descriptive statistics was first used to analyze these data, by tabulating the average values of the two area values in both the arterial and the portal venous phases.

The tables below show the tabulated average values of the areas in both phases.

**Table 2:** The average volume of the segmented tumors from both the AP and PVP.

| Patient | Arterial Avg. (cm <sup>3</sup> ) | Venous Avg. (cm <sup>3</sup> ) |
|---------|----------------------------------|--------------------------------|
| 1       | 2.125358125                      | 3.998260625                    |
| 2       | 58.48201375                      | 28.58909                       |
| 3       | 3.983966875                      | 4.463115625                    |
| 4       | 0.677465                         | 2.314268125                    |
| 5       | 4.49856375                       | 3.7184775                      |
| 6       | 0.131061875                      | 0.05736                        |
| 7       | 13.28473688                      | 20.60657563                    |
| 8       | 11.97801688                      | 11.69034625                    |
| 9       | 0.792245                         | 0.508279375                    |
| 10      | 0.69069625                       | 0.592025                       |
| 11      | 1.3645025                        | 1.34688875                     |
| 12      | 0.69090375                       | 0.3621375                      |
| 13      | 0.11345125                       | 0.087796875                    |
| 14      | 0.11345125                       | 0.079719375                    |
| 15      | 0.107154375                      | 0.054005625                    |
| 16      | 0.203751875                      | 0.18934675                     |
| 17      | 2.1237125                        | 1.729385625                    |
| 18      | 0.6008275                        | 0.664256875                    |
| 19      | 0.785410625                      | 0.664926875                    |

The mean values for both the arterial and the portal venous phases of the acquired image of the HCC tumors were used to determine the relevance through precision of individual data points collected. Furthermore, relevance of the data points collected for both phases of the acquired images was also determined by setting 0.1 as the maximum threshold deviation of these points from the mean value of both the arterial and the portal venous phases. The 0.1 which is a small number is just an arbitrary limit set for the data, in order to keep the data set concise and consistent. The tables 3- 4, shows the deviations from the mean value.

**Table 3:** Mean deviations for the dual volume measurements of the AP tumors.

| <b>Patient</b> | <b>Arterial Avg. (cm<sup>3</sup>)</b> | <b>Arterial 1 – Arterial Avg. (cm<sup>3</sup>)</b> | <b>Arterial 2 – Arterial Avg. (cm<sup>3</sup>)</b> |
|----------------|---------------------------------------|--|--|
| 1              | 2.125358125                           | -0.080961875                                       | 0.080961875  |
| 2              | 58.48201375                           | 0.21017625   | -0.21017625  |
| 3              | 3.983966875                           | 0.153365625  | -0.153365625                                       |
| 4              | 0.677465                              | -0.01408   | 0.01408  |
| 5              | 4.49856375                            | -0.03303375  | 0.03303375   |
| 6              | 0.131061875                           | 0.002334375  | -0.002334375                                       |
| 7              | 13.28473688                           | 0.016068125  | -0.016068125                                       |
| 8              | 11.97801688                           | 0.076320625  | -0.076320625                                       |
| 9              | 0.792245                              | 0.00710875   | -0.00710875  |
| 10             | 0.69069625                            | 0.0074625  | -0.0074625   |
| 11             | 1.3645025                             | 0.00494375   | -0.00494375  |
| 12             | 0.69090375                            | 0.00741625   | -0.00741625  |
| 13             | 0.11345125                            | -0.00741125  | 0.00741125   |
| 14             | 0.11345125                            | -0.00741125  | 0.00741125   |
| 15             | 0.107154375                           | -0.001714375                                       | 0.001714375  |
| 16             | 0.203751875                           | -0.029505625                                       | 0.029505625  |
| 17             | 2.1237125                             | -0.00538375  | 0.00538375   |
| 18             | 0.6008275                             | -0.00155625  | 0.00155625   |
| 19             | 0.785410625                           | 0.005585625  | -0.005585625                                       |

**Table 4:** Mean deviations for the dual volume measurements of the PVP tumors

| Patient | Avg. Venous (cm <sup>3</sup> ) | Venous 1 - Venous avg. (cm <sup>3</sup> ) | Venous 2 - Venous avg. (cm <sup>3</sup> ) |
|---------|--------------------------------|---|---|
| 1       | 3.998260625                    | -0.003589375                              | 0.003589375                               |
| 2       | 28.58909                       | 0.2105475                                 | -0.2105475                                |
| 3       | 4.463115625                    | 0.191465625                               | -0.191465625                              |
| 4       | 2.314268125                    | 0.023556875                               | -0.023556875                              |
| 5       | 3.7184775                      | 0.14648625                                | -0.14648625                               |
| 6       | 0.05736                        | -0.00133375                               | 0.00133375                                |
| 7       | 20.60657563                    | -0.151405625                              | 0.151405625                               |
| 8       | 11.69034625                    | 0.7341625                                 | -0.7341625                                |
| 9       | 0.508279375                    | 0.004145625                               | -0.004145625                              |
| 10      | 0.592025                       | -0.01575375                               | 0.01575375                                |
| 11      | 1.34688875                     | 0.02873625                                | -0.02873625                               |
| 12      | 0.3621375                      | -0.00618                                  | 0.00618                                   |
| 13      | 0.087796875                    | 0.009121875                               | -0.009121875                              |
| 14      | 0.079719375                    | -0.000618125                              | 0.000618125                               |
| 15      | 0.054005625                    | 0.002571875                               | -0.002571875                              |
| 16      | 0.18934675                     | -0.02439425                               | 0.02439425                                |
| 17      | 1.729385625                    | -0.121933125                              | 0.121933125                               |
| 18      | 0.664256875                    | -0.001945625                              | 0.001945625                               |
| 19      | 0.664926875                    | 0.005319375                               | -0.005319375                              |

Finally, a simple right tail paired sample t-test was performed on the both arterial and venous average HCC volume values to determine if or not there is a significant difference between them.

**Table 5:** Output of the computed simple right tail t-test of the AP and PVP liver tumor volumes.

| Patient | Avg. Arterial (cm <sup>3</sup> ) | Avg. Venous (cm <sup>3</sup> ) |
|---------|----------------------------------|--------------------------------|
| 1       | 2.125358125                      | 3.998260625                    |
| 2       | 58.48201375                      | 28.58909                       |
| 3       | 3.983966875                      | 4.463115625                    |
| 4       | 0.677465                         | 2.314268125                    |
| 5       | 4.49856375                       | 3.7184775                      |
| 6       | 0.131061875                      | 0.05736                        |
| 7       | 13.28473688                      | 20.60657563                    |
| 8       | 11.97801688                      | 11.69034625                    |
| 9       | 0.792245                         | 0.508279375                    |
| 10      | 0.69069625                       | 0.592025                       |
| 11      | 1.3645025                        | 1.34688875                     |
| 12      | 0.69090375                       | 0.3621375                      |
| 13      | 0.11345125                       | 0.087796875                    |
| 14      | 0.11345125                       | 0.079719375                    |
| 15      | 0.107154375                      | 0.054005625                    |
| 16      | 0.203751875                      | 0.18934675                     |
| 17      | 2.1237125                        | 1.729385625                    |
| 18      | 0.6008275                        | 0.664256875                    |
| 19      | 0.785410625                      | 0.664926875                    |

| t-Test: Paired Two Sample for Means |                         |                       |
|-------------------------------------|-------------------------|-----------------------|
|                                     | <i>Arterial average</i> | <i>Venous Average</i> |
| Mean                                | 5.407752105             | 4.300855914           |
| Variance                            | 179.6991232             | 60.48633936           |
| Observations                        | 19                      | 19                    |
| Pearson Correlation                 | 0.903738551             |                       |
| Hypothesized Mean Difference        | 0                       |                       |
| df                                  | 18                      |                       |
| t Stat                              | 0.670733493             |                       |
| P(T<=t) one-tail                    | 0.255452893             |                       |
| t Critical one-tail                 | 1.734063607             |                       |
| P(T<=t) two-tail                    | 0.510905787             |                       |
| t Critical two-tail                 | 2.10092204              |                       |

## DISCUSSION

Dual phase computed tomography imaging of the liver is often being used in the treatment evaluation and staging of liver tumors such as HCC during clinical trials. Hepatocellular carcinoma also known as primary liver carcinoma is a form of liver cancer that accounts for most liver cancers that is seen in the human population till date. A dual phase imaging protocol has become the standard method for imaging HCC tumors in the liver using CT due to the basic physiology of the liver in terms of its blood supply and distribution function. In this study, volume paradigm was used in the accessing the difference in the volume of both phases and potentially negating the usefulness of the portal venous phase in the imaging protocol. In assessing the differences in the volumes of both phases, an experimental design using volume paradigm was designed and used in assessing the difference in the volume of both phases and potentially negating the usefulness of one of the image acquisition phase during clinical trials. The objective of the experiment is determine if there is a statistical difference between the volumes of the arterial and venous acquired images of the same patient with focal HCC tumors in a randomly sampled population.

Descriptive statistics was first used in testing of the hypothesis for this study. The HCC tumors in both the arterial and portal venous phase of the acquired images for the 19 subjects in this study were manually segmented two times each within 24 hours. The segmentation was done twice on both phases of the image acquisition and the mean of the segmented areas subtracted from both volumes values of the segmented images in both phases of the acquired image in order to avert systematic errors and also limit the huge

fluctuations in the data set. The threshold value set for the deviation of the both data points in phase of the acquired image was at  $0.1\text{cm}^3$ , as it is believed to be a relatively small value based on the descriptive statistical parameters used in analyzing these dataset. The result of this statistical analysis as seen on table 5 indicates that the data collected from the segmentation of the HCC tumor in each phase of the image acquisition were similar and useful towards further analysis via inferential statistics.

The inferential statistics computed for the data between the volume of the tumor in both phases of the acquired images gave values for ( $t = 0.67$ ,  $P = 0.26$ ). Since the P value for the one tailed sample t test is greater than 0.05, the null hypothesis which presumes the equality of both the volumes of tumors acquired in the arterial and the portal venous phase to be true.

## CONCLUSION

The results of the paired t-test for this study went contrary to the underlying hypothesis for this experiment which presumes significant difference in the volume of the tumor of both the AP images compared to the PVP images. The patient populations that constitute the subject in which the data for this experiment was derived are adult population of different body mass index, with pathologically identified HCC tumors. Since the results of the experiment showed no significant difference in the volumes of HCC in AP and PVP images of a CT scan, it can be deduced that either phase can be used to measure tumor volume in the liver for clinical trial purpose. This is important as it limits the overall patient exposure to x-ray beams from the CT x-ray tube. This idea supports the core of the experiments hypothesis that assumes the removal of negligible phase of the imaging acquisition phase (either AP or PVP), as determined by a qualified physician during clinical trials only.

In conducting this research and evaluating the results of its statistically analyzed data, it can be deduced that the dual phase imaging of pathologically determined HCC will still be common place for clinical diagnosis. This is due to the sensitivity that the dual phase imaging provides in determining other non-vascular tumors that may have being missed during earlier diagnosis of patients.

## REFERENCES

- Bae, Kyongtae T. "Intravenous Contrast Medium Administration and Scan Timing at CT: Considerations and Approaches 1." *Radiology* 256.1 (2010): 32-61.
- Baron, R. L. "Understanding and optimizing use of contrast material for CT of the liver." *AJR. American journal of roentgenology* 163.2 (1994): 323-331.
- Baron, Richard L., et al. "Hepatocellular carcinoma: evaluation with biphasic, contrast-enhanced, helical CT." *Radiology* 199.2 (1996): 505-511.
- Bonaldi, Vincent M., et al. "Helical CT of the liver: value of an early hepatic arterial phase." *Radiology* 197.2 (1995): 357-363.
- Brink, J. A., Heiken, J. P., Forman, H. P., Sagel, S. S., Molina, P. L., & Brown, P. C. (1995). Hepatic spiral CT: reduction of dose of intravenous contrast material. *Radiology*, 197(1), 83-88.
- Bruix, Jordi, and Morris Sherman. "Management of hepatocellular carcinoma: an update." *Hepatology* 53.3 (2011): 1020-1022.
- Foley, W. Dennis, et al. "Multiphase hepatic CT with a multirow detector CT scanner." *American Journal of Roentgenology* 175.3 (2000): 679-685.
- Frederick, M. Gena, et al. "Timing of parenchymal enhancement on dual-phase dynamic helical CT of the liver: how long does the hepatic arterial phase predominate?." *AJR. American journal of roentgenology* 166.6 (1996): 1305-1310.
- Hamer, Okka W., et al. "Technology insight: advances in liver imaging." *Nature clinical practice Gastroenterology & hepatology* 4.4 (2007): 215-228.
- Hollett, M. D., et al. "Dual-phase helical CT of the liver: value of arterial phase scans in the detection of small ( $\leq$  1.5 cm) malignant hepatic neoplasms." *AJR. American journal of roentgenology* 164.4 (1995): 879-884.
- Hwang, Geum Ju, et al. "Nodular hepatocellular carcinomas: detection with arterial-, portal-, and delayed-phase images at spiral CT." *Radiology* 202.2 (1997): 383-388.
- Ichikawa, Tomoaki, et al. "Hypervascular hepatocellular carcinoma: can double arterial phase imaging with multidetector CT improve tumor depiction in the cirrhotic liver?." *American Journal of Roentgenology* 179.3 (2002): 751-758.
- Kambadakone, Avinash R., and Dushyant V. Sahani. "Body perfusion CT: technique, clinical applications, and advances." *Radiologic Clinics of North America* 47.1 (2009): 161-178.

- Laghi, Andrea, et al. "Hepatocellular Carcinoma: Detection with Triple-Phase Multi-Detector Row Helical CT in Patients with Chronic Hepatitis 1." *Radiology* 226.2 (2003): 543-549.
- Levy, Izhar, et al. "Resection of hepatocellular carcinoma without preoperative tumor biopsy." *Annals of surgery* 234.2 (2001): 206.
- Ma, Xiaozhou, et al. "Optimal arterial phase imaging for detection of hypervascular hepatocellular carcinoma determined by continuous image capture on 16-MDCT." *American Journal of Roentgenology* 191.3 (2008): 772-777.
- Miles, K. A. "Perfusion CT for the assessment of tumour vascularity: which protocol?." (2014).
- Miles, K. A. "Tumour angiogenesis and its relation to contrast enhancement on computed tomography: a review." *European journal of radiology* 30.3 (1999): 198-205.
- Miller, FrankH, et al. "Using triphasic helical CT to detect focal hepatic lesions in patients with neoplasms." *AJR. American journal of roentgenology* 171.3 (1998): 643-649.
- Mitsuzaki, Katsuhiko, et al. "Multiple-phase helical CT of the liver for detecting small hepatomas in patients with liver cirrhosis: contrast-injection protocol and optimal timing." *AJR. American journal of roentgenology* 167.3 (1996): 753-757.
- Murakami, Takamichi, et al. "Hypervascular Hepatocellular Carcinoma: Detection with Double Arterial Phase Multi-Detector Row Helical CT 1." *Radiology* 218.3 (2001): 763-767.
- Nino-Murcia, Matilde, et al. "Focal Liver Lesions: Pattern-based Classification Scheme for Enhancement at Arterial Phase CT 1." *Radiology* 215.3 (2000): 746-751.
- Oliver 3rd, J. H., and Richard L. Baron. "Helical biphasic contrast-enhanced CT of the liver: technique, indications, interpretation, and pitfalls." *Radiology* 201.1 (1996): 1-14.
- Oliver 3rd, J. H., et al. "Detecting hepatocellular carcinoma: value of unenhanced or arterial phase CT imaging or both used in conjunction with conventional portal venous phase contrast-enhanced CT imaging." *AJR. American journal of roentgenology* 167.1 (1996): 71-77.
- Oliver 3rd, J. H., et al. "Hypervascular liver metastases: do unenhanced and hepatic arterial phase CT images affect tumor detection?." *Radiology* 205.3 (1997): 709-715.

- Platero, Carlos, et al. "Liver segmentation for hepatic lesions detection and characterisation." *Biomedical Imaging: From Nano to Macro, 2008. ISBI 2008. 5th IEEE International Symposium on*. IEEE, 2008.
- Sahani, D., et al. "Preoperative Vascular Evaluation Of The Liver For Neoplasms With Multislice Computed Tomography: Technique And Results." *AJR* 179.1 (2002): 53-9.
- Sahani, Dushyant V., et al. "Advanced Hepatocellular Carcinoma: CT Perfusion of Liver and Tumor Tissue—Initial Experience 1." *Radiology* 243.3 (2007): 736-743.
- Schoellnast, Helmut, et al. "High-concentration contrast media in multiphase abdominal multidetector-row computed tomography: effect of increased iodine flow rate on parenchymal and vascular enhancement." *Journal of computer assisted tomography* 29.5 (2005): 582-587.
- Smeets, Dirk, et al. "Semi-automatic level set segmentation of liver tumors combining a spiral-scanning technique with supervised fuzzy pixel classification." *Medical image analysis* 14.1 (2010): 13-20.
- Takayasu, K., et al. "CT diagnosis of early hepatocellular carcinoma: sensitivity, findings, and CT-pathologic correlation." *AJR. American journal of roentgenology* 164.4 (1995): 885-890.
- Van Hoe, Lieven, et al. "Dual-phase helical CT of the liver: value of an early-phase acquisition in the differential diagnosis of noncystic focal lesions." *AJR. American journal of roentgenology* 168.5 (1997): 1185-1192.
- Yim, Peter J., and David J. Foran. "Volumetry of hepatic metastases in computed tomography using the watershed and active contour algorithms." *Computer-Based Medical Systems, 2003. Proceedings. 16th IEEE Symposium*. IEEE, 2003.
- Zhou, Jia-Yin, et al. "Liver tumour segmentation using contrast-enhanced multi-detector CT data: performance benchmarking of three semiautomated methods." *European radiology* 20.7 (2010): 1738-1748.

## CURRICULUM VITAE

**Ehimen Edward. Aisaborhale**

[ehi\\_aisa@yahoo.com](mailto:ehi_aisa@yahoo.com)

38 Pleasant street, Floor1

Randolph, MA 02368

Born 1983

313-898-4660

---

### **Summary:**

- Detailed-oriented, self-motivated, and highly-organized professional, offering years of progressive industrial experience in the pharmaceutical and clinical research industries. Qualified with outstanding verbal and written communication skills necessary in establishing long-term relationships with all levels individual with diverse background.
- Adept at grasping new processes, procedures, resources, and services related to any clinical service population quickly. Demonstrate appreciation for diversity and express sincere passion and interest in pharmaceuticals and bio-medicine.
- Acknowledged for decisive leadership and professionalism with a positive, can-do attitude and commitment to excellence.
- Equipped with exceptional planning, prioritizing, and goal-setting skills.
- Proficient in MS Office Suite (Word, Excel, Publisher, Outlook, and PowerPoint and more).

### **Education:**

- **BS, Biochemistry, minor in Philosophy**  
University of Detroit Mercy, MI.  
April 2011.

### **Experience:**

- Athinuola Martinos Center for Biomedical Imaging  
(Massachusetts General Hospital – Harvard University/MIT Science and Technology Program)  
  
Radiochemist/Radiopharmacy Research Technician: September 2012 – Present

- cGMP compounding of  $^{11}\text{C}$ ,  $^{18}\text{F}$ ,  $^{64}\text{Cu}$ ,  $^{15}\text{O}$  labelled radiotracers and radiopharmaceuticals accordingly using semi-automated Synthesis boxes.
- Quality control of in-house produced radiotracers and radiopharmaceuticals using chemistry analytical tools such as HPLC, GC-MS and others in accordance with relevant sections of the United States Pharmacopeia compendium (USP).
- Development, validation and testing of new radiotracers produced in-house for review by the Radioactive Drug Research Committee (RDRC) and the U.S. Food and Drug Administration (FDA).
- Components testing of materials used in the cGMP production of radiotracers based on set standard specification requirements.
- Clean room operation for the aseptic sterile filtration of in-house produced radiotracers.
- Process and analyze radioactive blood of experimental subject post-injection of in-house produced radiotracers.
- Train new employees and technicians on proper use of automated synthesis unit and proper radiation protection procedures.
- Inventory control of components used in the cGMP production of radiotracers.
- Compilation and documentation of batch records based on good documentation practices.
- Assist investigators in the preparation and review of new IND for new drug studies.
- Preparation of CAPA reports based on good document practice (GDP).
- Write and constantly review standard operating procedures (SOP) for preparation and compounding of in-house produced radiotracers.

#### Enanta Pharmaceuticals.

Temp Scientist: August 2011 – February 2012

- Utilized various technical software's such as Cispro, Activity Base, Chem-Draw and others, to analyze, draw, register and catalog potential drug samples into an existing database.
- Daily used inventory control measures and software to distribute and allocate chemicals for researchers.
- Supported medicinal chemistry researcher through the formulations and analysis of potential drug compounds, using various analytical tools such as HPLC, GC-MS and LC-MS in the laboratory.

#### ○ **Undergraduate Research Student in organic synthesis.**

University of Detroit Mercy

August 2009- May 2010

- Was part of a research team that develop phosphorous containing pseudo-peptide folate analogs which are potential cancer inhibitors. These analogs

can mimic the tetrahedral intermediate formed ATP-dependent reaction catalyzed folypolyglutamate synthetase (FPGS). This analogs are competitive inhibitors for recombinant human cystolic FPGS.

**Software competence:**

- Highly competent in Microsoft office package e.g (excel, word, outlook, PowerPoint etc.) and Linux.

**Campus Involvement:**

- **Residential Assistant – University of Detroit Mercy**
  - Help promote student activities for residential students and render appropriate support to student as needed on school property.